Laminographic imaging using synchrotron radiation - challenges and opportunities

Lukas Helfen, Feng Xu, Heikki Suhonen, Peter Cloetens, Tilo Baumbach

Journal of Physics: Conference Series **425** (2013) 192025 doi:10.1088/1742-6596/425/19/192025

Laminographic imaging using synchrotron radiation – challenges and opportunities

Lukas Helfen[1,2], Feng Xu[1], Heikki Suhonen[2], Peter Cloetens[2], Tilo Baumbach[1]

[1] ANKA Light Source / Institute for Photon Science and Synchrotron Radiation, Karlsruhe Institute of Technology, PO Box 3640, D-76021 Karlsruhe, Germany
[2] European Synchrotron Radiation Facility (ESRF), BP220, F-38043 Grenoble cedex, France

E-mail: lukas.helfen@kit.edu

Abstract. Synchrotron-radiation computed laminography (SRCL) was developed as a nondestructive three-dimensional (3D) imaging technique for flat and laterally extended objects. Complementing the established method of computed tomography, SRCL is based on the inclination of the tomographic axis with respect to the incident x-ray beam by a defined angle. Its ability for 3D imaging of regions of interest in flat specimens was demonstrated in various fields of investigation, *e.g.* in nondestructive testing, material science and life sciences. We introduce the principles of the method and report on the latest developments of SRCL. The experimental set-ups at the ESRF beamlines ID19 and ID22NI are dedicated to 3D micro- and nano-scale imaging, respectively, utilising different contrast modes including absorption, phase contrast and fluorescence. Selected examples from materials science outline the potential of the method for an unparalleled nondestructive 3D characterisation of flat specimens.

1. Introduction

Despite numerous publications which have appeared in several research fields, laminographic imaging using synchrotron radiation (SR) can still be considered as a relatively new technique, at least if one compares the situation to the now well established technique of computed tomography (CT) [1, 2]. First publications on synchrotron-radiation computed laminography (SR-CL) appeared around 2005 [3, 4] and described a method that was primarily developed for nondestructive imaging and inspection of microsystem and microelectronic devices [5, 6]. These applications take advantage of the high collimation of synchrotron beams and the inherently large distance towards the source (which eliminates the potential risk of the collision of the specimen with the source enclosure) but require high-resolution imaging detectors.

A significant advantage of using synchrotron over laboratory radiation (*e.g.* as provided by conventional x-ray tubes) consists in the access to different imaging contrast modes. A prominent example is the availability of phase contrast [7] due to a partially coherent wavefield at the specimen position which enables edge-enhancing laminographic imaging [8, 9]. This opens up a vast range of new application fields for laminographic imaging, *e.g.* in cultural heritage studies [8], in engineering [10] or in the materials sciences [11, 12]. Using more refined phase retrieval techniques, see *e.g.* [13, 14], different materials can be distinguished [9, 15] (as opposed to only the interfaces between them) which again broadens the range of application.

Recently developed contrast modes use x-ray diffraction [16] to image crystal defects or the x-ray fluorescence signal for laminographic imaging of the spatial distribution of chemical elements [17]. Especially the latter might have a considerable impact since it enables 3D imaging of trace elements in life science studies on large specimens [18].

In this paper, we briefly describe the imaging geometry and different contrast modalities. Section 2 is devoted to imaging in the parallel-beam geometry where most of the work has been carried out. Section 3 describes more recent developments employing x-ray focussing. For both geometries, a survey of research fields already addressed is given.

2. Laminographic imaging in the parallel-beam geometry

Laminographic imaging is commonly applied in device testing [19] and in medical imaging where it is also termed "tomosynthesis" [20]. There exist different acquisition geometries, and early approaches simply integrate an image during a synchronised motion of the source and detector in order to blur out specimen structures which are not situated on the so-called focal plane of the apparatus. Other acquisition schemes use a divergent (fan- or cone-beam) geometry to acquire the different projection directions in separate images which are combined in a reconstruction step to yield cross-sectional or 3D images. The latter acquisition schemes cannot be realised at typical synchrotron imaging set-ups since, due to the long distance between source and experimental station, they usually operate in the parallel-beam geometry [21]. Since the magnification is close to one even if the detector is positioned some meters from the specimen, the imaging resolution is limited by the detector resolution. In a trade-off between (energy-dependent) detection efficiency, counting time and spatial resolution, approximately 0.5 μm resolution can be achieved in practice via indirect detection schemes at pixel sizes around 0.2 μm.

Like synchrotron CT, synchrotron CL [3] employs a source and a 2D pixel detector which are both stationary (*i.e.* neither translated nor rotated), see Fig. 1. As a result, different projection images need to be acquired under rotation of the specimen. Using different projection images it was almost obvious to include (like in CT imaging) an adapted projection filtering step in order to dampen over-represented low spatial frequencies [22] in the reconstructed images. The image acquisition scheme shown is relatively easy to implement, allows (due to the requirement of only one rotation) high spatial and temporal resolutions to be attained and, combined with projection filtering, provides a relatively balanced reproduction of the spatial frequencies despite the missing data in the specimen's Fourier domain [20]. The principal differences compared to synchrotron CT are that the rotation axis (see Fig. 1) is inclined at an angle $\theta < 90°$ with respect to the direction of the optical axis and only a limited region of interest (ROI) is imaged inside the laterally extended specimen. Different application cases have been identified [22, 23]

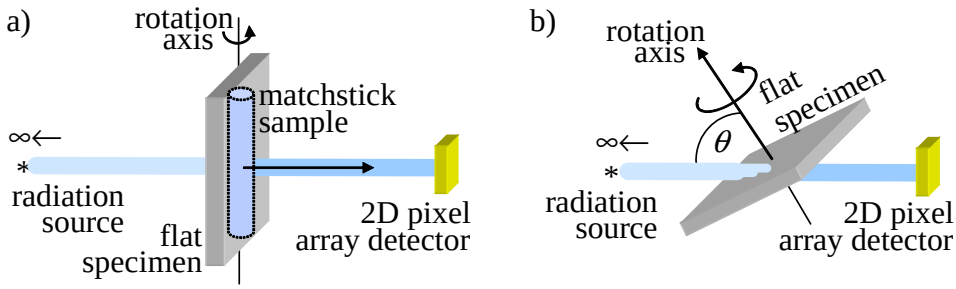

Figure 1. Comparison of the scanning geometries of SR-CT and SR-CL in the parallel-beam geometry. CT is optimised towards matchstick-like specimens (a) while CL is adapted to plate-like specimens (b) where only a limited ROI around the rotation axis is scanned.

where this data acquisition scheme provides more reliable projection data than limited-angle CT (*i.e.* the case when a complete plate-like specimen is scanned using CT, see Fig. 1a). This advantage and the ability to achieve μm resolution could be successfully applied in a number of studies including materials science [11, 24, 25] or device engineering [26].

More traditional digital tomosynthesis methods (*i.e.* without projection filtering) using a scanning geometry similar to limited-angle CT with detector rotation during a scan [27] and variants with a stationary detector were also reported [28]. First attempts involving both a rotated specimen and detector [29] using dark-field imaging indicated potential applications in medical imaging.

As already stated, the degree of coherence of synchrotron radiation enables phase-contrast imaging based on simple propagation of the wavefield after passing the specimen. Different approaches (which use differently processed projection data but the same 3D reconstruction algorithm based on filtered backprojection [30]) are illustrated in Fig. 2 by the example of an open-porous diffusion layer mainly made from carbon (see 3D rendering in a): imaging in the so-called edge-detection regime with a single relatively low propagation distance where only the outlines of the microstructural constituents (here interconnected spheres) appear (b), using a single-distance phase retrieval algorithm [14] (c) or using a holographic multi-distance approach [13] (d). In the latter two cases one sees contrast corresponding to different materials (*i.e.* carbon and air). The profiles (e) allow one to assess the adaptedness of the different approaches: the edge-detection regime (b) only emphasises the interfaces between different materials which results in hollow spheres while the phase-retrieval approaches (c) and (d) reflect the true geometry (filled spheres). For this particular example we see that the holographic approach possibly yields a higher resolution (steeper edges) than the single-distance approach. These phase-contrast possibilities have contributed considerably to provide 3D micro-imaging of flat specimens in a variety of scientific studies, ranging from artwork studies [31] over paleontology [32] to materials science [33].

Very recently, phase-contrast laminography has also been realised via Talbot interferometry [34, 35, 36] where a grating interferometer serves for wavefront sensing. Grating interferometry can provide – depending on the Talbot order chosen – very high sensitivity for phase imaging [37] and also allows for using the scattering properties [38] of the microstructure as an additional contrast mode.

Direct sensitivity towards specific chemical elements could be obtained via substraction imaging above and below an absorption edge (*e.g.* K-edge) of the element or via fluorescence imaging decribed in the following section.

3. Laminography with spatial resolution towards the deep sub-μm scale

It is a challenge to provide laminographic imaging with spatial resolutions at the deep sub-μm and nm length scale. As for other 3D imaging modalities like CT, a major difficulty consists in achieving the required resolution in the projection images, *e.g.* using devices for reproducible and stable focussing of the x rays. Particularly for CL, another challenge is to achieve a satisfactory precision for the specimen rotation (around an inclined axis), which could again reduce the spatial resolution.

Different approaches have been explored recently. Using 2D scanning techniques of an object in the focal point of a focused x-ray beam, spatial resolutions in the reconstructed images of around 3 μm [17] and 0.5 μm [18] have been reported. Obviously, the combination of such 2D scanning with laminography is very time-consuming and therefore restricted to low-definition 3D images in the order of 100^3 voxels. Full-field laminographic imaging with a spatial resolution of around 0.5 μm has been demonstrated on a biological specimen by means of an x-ray microscope configuration with Fresnel zone plates as condenser and objective lenses [39].

Using a projection microscopy approach of an x-ray beam nano-focused via a Kirkpatrick-

Baez device [18], a spatial resolution of around 130 nm has been measured. This approach requires phase-retrieval techniques to be applied but it can be combined in a rather straightforward way with fluorescence scanning. For phase imaging, simply translating the specimen along the optical axis permits zooming into the region of interest with adjustable spatial resolution [40]. Fluorescence imaging with variable stepping resolution is performed in the focal plane, allowing for correlative imaging of structure and composition. The following example of an AA8079 Al alloy foil is used to demonstrate the ability to detect and identify the constituent elements of second-phase particles like intermetallics inside the aluminium matrix.

The hololaminography image was obtained via full-field projection microscopy imaging (effective pixel size 60 nm) while the projections of the fluorescence image were acquired via raster scanning microscopy of the specimen in the x-ray focal plane. The hololaminography reconstruction reveals plenty of dense particles inside the Al foil (see Fig. 3) which cannot be identified in terms of chemical composition. By combining the fluorescence results into the phase contrast images, we see that the particles are mainly composed of Fe, Ni and Cu, with a varying composition in the different particles.

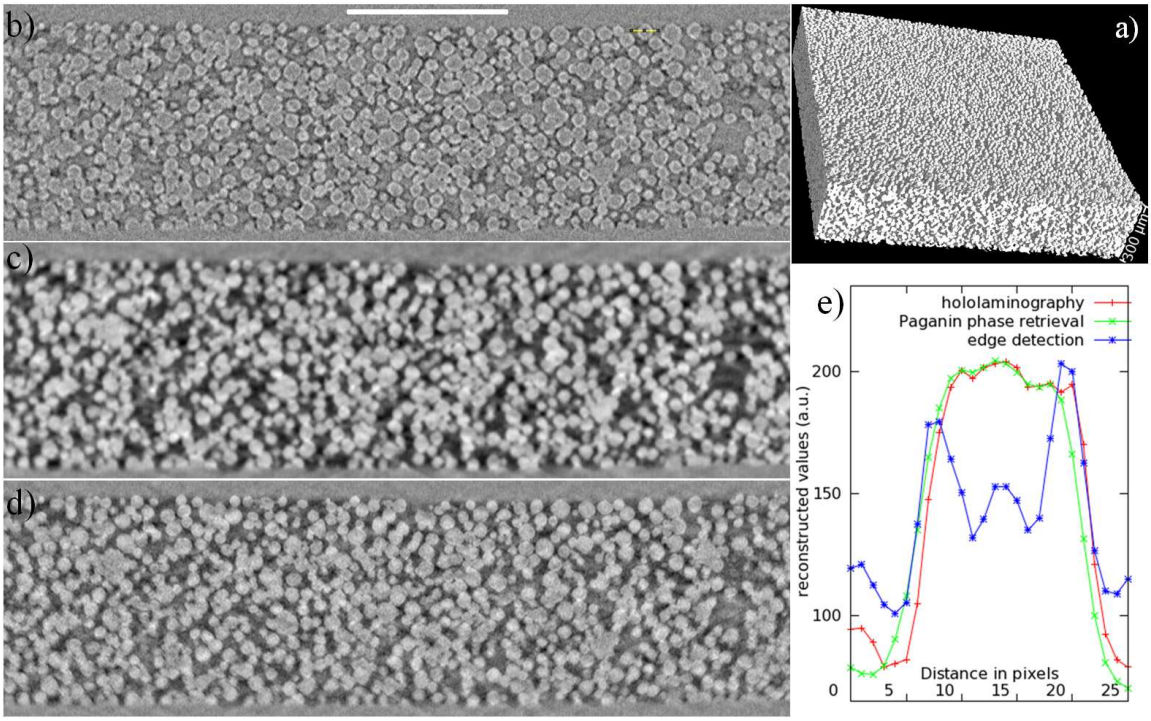

Figure 2. Comparison of different propagation-based phase-contrast modes for laminographic imaging of an open-porous diffusion layer, see the 3D rendering in (a). The through-plane slices (b) and (c) were reconstructed from the same data, 900 projections acquired at ESRF beamline ID19 at a single specimen-detector distance of 0.03 m: direct reconstruction (b) and employing a single-distance phase-retrieval method (c) based on D. Paganin's approach [14]. The scale bar is 300 μm long. The slice (d) produced by hololaminography [13] uses three additional projection data sets at the distances 0.045, 0.105 and 0.215 m. The plot (e) compares profiles through the sphere along the 35 μm long line shown in (b). Axis inclination θ=60°, x-ray energy 20.5 keV, voxel size 1.4 μm. Adapted from [9].

4. Summary

Despite being a relatively new technique, synchrotron laminography has been applied in various research fields where flat, plate-like objects are prevalent. Imaging in the parallel-beam geometry yields spatial resolutions in the order of 1 μm which in many application fields is sufficient to get new insight about the specimens or processes. X-ray microscopy techniques allow one to go towards the deep sub-μm scale. Future sources or focussing devices will certainly allow one to go to even higher spatial resolutions. Nanolaminography allows one to obtain 3D volume images zoomed with adjustable spatial resolution into a macroscopically large specimen. This allows one, for instance, to focus in heterogeneous specimens onto zones which are highly different from the surroundings. The high spatial resolutions and the combination with fluorescence imaging may enable new studies especially in the life sciences but also in technologically oriented materials and engineering sciences.

Acknowledgments

The authors would like to thank W. Ludwig for his precious help in the implementation of algebraic reconstruction techniques and P. Bernard for developing the specimen positioning mechanics. The ESRF is acknowledged for provision of beam time via proposal MI-979.

References

[1] Grodzins L 1983 *Nuclear Instruments and Methods in Physics Research* **206** 541 – 545
[2] Flannery P, Deckmann H, Roberge W and DAmico K 1987 *Science* **237** 1439–1444
[3] Helfen L, Baumbach T, Mikulík P, Kiel D, Pernot P, Cloetens P and Baruchel J 2005 *Appl. Phys. Lett.* **86** 071915
[4] Helfen L, Baumbach T, Pernot P, Mikulík P, DiMichiel M and Baruchel J 2006 *Proc. SPIE* **6318** 63180N

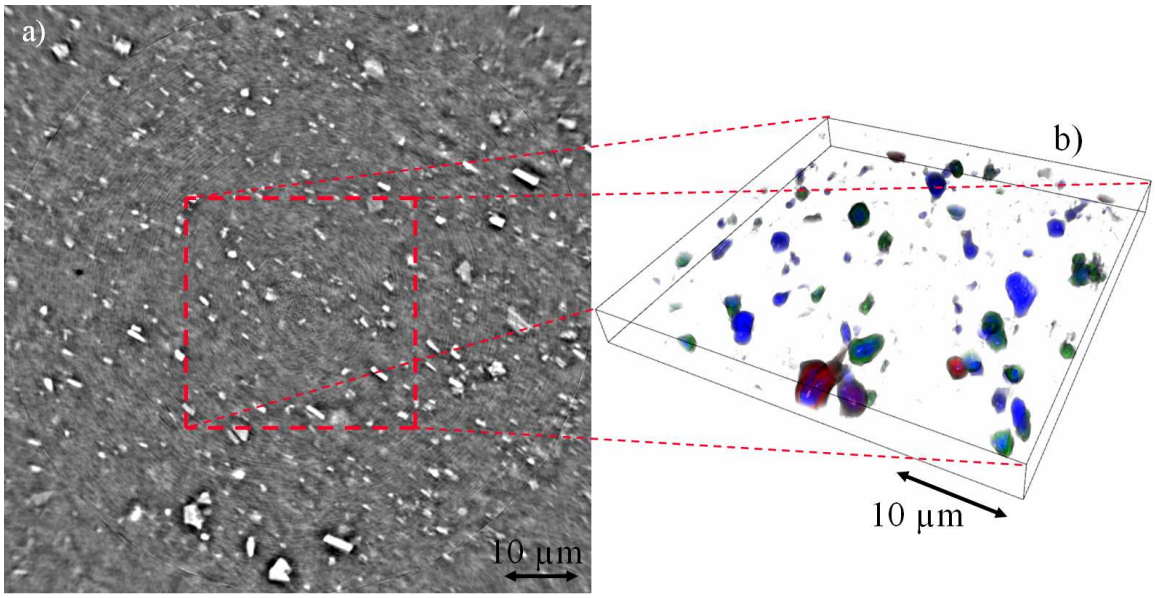

Figure 3. Combined phase and fluorescence imaging of an ROI inside an AA8079 Al alloy foil performed at ESRF beamline ID22NI at 17.5 keV with a focus size smaller than 100 nm. The hololaminography slice (a) reconstructed by filtered backprojection from 1499 projections using an effective pixel size of 60 nm is proportional to the electron density. Fluorescence laminography 3D volume (b) reconstructed by algebraic reconstruction from 64 projections of 50×50 μm^2 size (0.5 μm step size). Colour coding: blue - Fe, red - Ni, green - Cu. Axis inclination is $\theta=60°$.

[5] Helfen L, Myagotin A, Pernot P, DiMichiel M, Mikulík P, Berthold A and Baumbach T 2006 *Nucl. Inst. Meth. A* **563** 163–166
[6] Helfen L, Myagotin A, Rack A, Pernot P, Mikulík P, Michiel M D and Baumbach T 2007 *phys. stat. sol. (a)* **204** 2760–2765
[7] Cloetens P, Pateyron-Salomé M, Buffière J Y, Peix G, Baruchel J, Peyrin F and Schlenker M 1997 *J. Appl. Phys.* **81** 5878–5885
[8] Krug K, Porra L, Coan P, Wallert A, Dik J, Coerdt A, Bravin A, Elyyan M, Reischig P, Helfen L and Baumbach T 2008 *J. Synchrotron Radiat.* **15** 55–61
[9] Helfen L, Baumbach T, Cloetens P and Baruchel J 2009 *Appl. Phys. Lett.* **94** 104103
[10] Maurel V, Soulignac R, Helfen L, NGuyen F, Morgeneyer T, Koster A and Rémy L Three-dimensional damage evolution measurement in TBC using synchrotron laminography *Oxidation of Metals* in press
[11] Moffat A J, Wright P, Helfen L, Baumbach T, Johnson G, Spearing S M and Sinclair I 2010 *Scripta Mater.* **62** 97–100
[12] Helfen L, Morgeneyer T F, Xu F, Mavrogordato M N, Sinclair I, Schillinger B and Baumbach T 2012 *Int. J. Mater. Res.* **103** 170–173
[13] Cloetens P, Ludwig W, Baruchel J, van Dyck D, van Landuyt J, Guigay J and Schlenker M 1999 *Appl. Phys. Lett.* **75** 2912
[14] Paganin D, Mayo S C, Gureyev T E, Miller P R and Wilkins S W 2002 *J. Microscopy* **206** 33–40
[15] Xu F, Helfen L, Moffat A J, Johnson G, Sinclair I and Baumbach T 2010 *J. Synchrotron Radiat.* **17** 222–226
[16] Hänschke D, Helfen L, Altapova V, Danilewsky A and Baumbach T Three-dimensional imaging of dislocations by X-ray diffraction laminography *Appl. Phys. Lett.* in press
[17] Watanabe N, Hoshino M, Yamamoto K, Aoki S, Takeuchi A and Suzuki Y 2009 *Journal of Physics: Conference Series* **186** 012022
[18] Xu F, Helfen L, Suhonen H, Elgrabli D, Bayat S, Reischig P, Baumbach T and Cloetens P 2012 *PLoS ONE* **7** e50124
[19] Zhou J, Maisl M, Reiter H and Arnold W 1996 *Appl. Phys. Lett.* **68(24)** 3500–3502
[20] Dobbins III J T and Godfrey D J 2003 *Phys. Med. Biol.* **48** R65–R106
[21] Weitkamp T, Tafforeau P, Boller E, Cloetens P, Valade J P, Bernard P, Peyrin F, Ludwig W, Helfen L and Baruchel J 2010 *AIP Conference Proceedings* vol 1234 ed Garrett R, Gentle I, Nugent K and Wilkins S pp 83–86
[22] Helfen L, Myagotin A, Mikulík P, Pernot P, Voropaev A, Elyyan M, Michiel M D, Baruchel J and Baumbach T 2011 *Review of Scientific Instruments* **82** 063702 (pages 8)
[23] Xu F, Helfen L, Baumbach T and Suhonen H 2012 *Opt. Express* **20** 794–806
[24] Maurel V, Helfen L, NGuyen F, Koster A, Michiel M D, Baumbach T and Morgeneyer T 2012 *Scripta Mater.* **66** 471 – 474
[25] Morgeneyer T, Helfen L, Mubarak H and Hild F 2013 *Exp. Mech.* in press, DOI:10.1007/s11340–012–9660–y
[26] Tian T, Xu F, Han J K, Choi D, Cheng Y, Helfen L, Michiel M D, Baumbach T and Tu K N 2011 *Appl. Phys. Lett.* **99** 082114
[27] Shimao D, Kunisada T, Sugiyama H and Ando M 2007 *Jpn. J. Appl. Phys.* **46** L608–L610
[28] Maksimenko A, Yuasa T, Ando M and Hashimoto E 2007 *Appl. Phys. Lett.* **91** 234108
[29] Shimao D, Kunisada T, Sugiyama H and Ando M 2008 *Eur. J. Radiol.* **68** S27 – S31
[30] Myagotin A, Voropaev A, Helfen L, Hänschke D and Baumbach T Fast volume reconstruction for parallel-beam computed laminography by filtered backprojection, manuscript submitted
[31] Dik J, Reischig P, Krug K, Wallert A, Coerdt A, Helfen L and Baumbach T 2009 *J. Am. Inst. Conserv.* **48** 185–197
[32] Houssaye A, Xu F, Helfen L, Buffrénil V D, Baumbach T and Tafforeau P 2011 *J. Vertebr. Paleontol.* **31** 2–7
[33] Morgeneyer T, Helfen L, Sinclair I, Proudhon H, Xu F and Baumbach T 2011 *Scripta Mater.* **65** 1010 – 1013
[34] Harasse S, Hirayama N, Yashiro W and Momose A 2010 *Proc. SPIE* **7804** 780411
[35] Harasse S, Yashiro W and Momose A 2011 *Opt. Express* **19** 16560–16573
[36] Altapova V, Helfen L, Myagotin A, Hänschke D, Moosmann J, Gunneweg J and Baumbach T 2012 *Opt. Express* **20** 6496–6508
[37] Weitkamp T, Diaz A, David C, Pfeiffer F, Stampanoni M, Cloetens P and Ziegler E 2005 *Opt. Express* **13** 6296–6304
[38] Altapova V, Helfen L, Butzer J, Moosmann J, Hänschke D, Monninger S, Frey E and Baumbach T Multiple contrast laminography, manuscript submitted
[39] Hoshino M, Uesugi K, Takeuchi A, Suzuki Y and Yagi N 2011 *Review of Scientific Instruments* **82** 073706
[40] Mokso R, Cloetens P, Maire E, Ludwig W and Buffière J Y 2007 *Appl. Phys. Lett.* **90** 144104